

# Effect of lithium borate coating on the electrochemical properties of LiCoO<sub>2</sub> electrode for lithium-ion batteries

Victor D. Zhuravlev<sup>a</sup> , Ksenia V. Nefedova<sup>a\*</sup> , Elizaveta Yu. Evshchik<sup>b</sup> ,  
Elena A. Sherstobitova<sup>a</sup> , Valery G. Kolmakov<sup>b</sup> , Yury A. Dobrovolsky<sup>b</sup> ,  
Natalia M. Porotnikova<sup>a</sup> , Andrey V. Korchun<sup>b</sup> , Anna V. Shikhovtseva<sup>b</sup> 



a: Institute of Solid State Chemistry, Ural Branch of the Russian Academy of Sciences,  
91 Pervomaiskaya St., Ekaterinburg, 620990, Russia

b: Institute of Problems of Chemical Physics, Russian Academy of Sciences,  
1 Ac. Semenov ave, Chernogolovka, Moscow region, 142432, Russia

\* Corresponding author: nefedova@ihim.uran.ru, ksenia\_nef@rambler.ru

This article belongs to the regular issue.

© 2021, The Authors. This article is published in open access form under the terms and conditions of the Creative Commons Attribution (CC BY) license (<http://creativecommons.org/licenses/by/4.0/>).

## Abstract

The effect of a protective coating of fused lithium borate, Li<sub>3</sub>BO<sub>3</sub>, on the physicochemical and electrochemical characteristics of LiCoO<sub>2</sub> has been studied. A cathode material produced by the SCS method using binary organic fuel, glycine and citric acid. The influence of the experiment conditions on the morphology, crystal structure and specific surface of lithium cobaltite was studied. Electrochemical testing of LiCoO<sub>2</sub>·nLi<sub>3</sub>BO<sub>3</sub> samples, n = 5 and 7 mass %, has been performed in the cathode Li|Li<sup>+</sup>-electrolyte|LiCoO<sub>2</sub>·nLi<sub>3</sub>BO<sub>3</sub> half-cell using 1M LiPF<sub>6</sub> in EC/DMC mixture (1:1) as electrolyte in the 2.7–4.3 V range at normalized discharge current C/10, C/5, C/2. The maximal initial discharge capacity of 185 mAh/g was detected for the samples with 5 mass % Li<sub>3</sub>BO<sub>3</sub>. The coulomb efficiency of optimal materials in the 40<sup>th</sup> cycle was 99.1%.

## Keywords

lithium-ion batteries  
lithium cobalt oxide  
solution combustion synthesis  
Li<sub>3</sub>BO<sub>3</sub> protective coating

Received: 13.10.2020

Revised: 18.11.2020

Accepted: 26.11.2020

Available online: 21.12.2020

## 1. Introduction

Lithium cobaltite LiCoO<sub>2</sub> (LCO) is used as a cathode material since 1990, and in spite of the appearance of such promising cathode materials as LiNi<sub>1/3</sub>Mn<sub>1/3</sub>Co<sub>1/3</sub>O<sub>2</sub> (NMC), LiNi<sub>0.8</sub>Co<sub>0.15</sub>Al<sub>0.05</sub>O<sub>2</sub> (NCA), LiMn<sub>2</sub>O<sub>4</sub> (LMO) etc. it is still employed as a component of lithium-ion batteries (LIB) with low discharge rates in portable gadgets [1]. Chemical interaction between the electrolyte and the cathode material leads to non-recoverable losses of lithium cations reduced service lifetime and accelerated capacity failure of LIB. The manufacturers of LIB materials try to eliminate this effect by decreasing the specific surface of dispersed materials, by using microgranulation processes or applying modifying coatings on cathode material particles, protecting them from the action of acid fluorine-containing components of electrolyte. In particular, Al<sub>2</sub>O<sub>3</sub>, ZrO<sub>2</sub>, ZnO, SiO<sub>2</sub>, TiO<sub>2</sub> and other oxides are used as protective coatings [2–5]. Recently appeared publications reporting the application of glasses and boron and lithium based oxides as coatings [5–7]. A. Nagasubramanian et al. [6] studied the effect of LiBO<sub>2</sub> coating on the electrochemical performance

of orthorhombic LiMnO<sub>2</sub> cathode. ShuangYuan Tan et al. [7] showed that using glass-coated NMC/Li<sub>2</sub>O·B<sub>2</sub>O<sub>3</sub> can increase the discharge capacity retention of the cathode from 22.5% to 57.8% at -40 °C. Among compounds in the Li<sub>2</sub>O-B<sub>2</sub>O<sub>3</sub> system, lithium borate Li<sub>3</sub>BO<sub>3</sub> should be noted [8–10]. It has the lowest melting temperature, 715±15 °C [11], which allows applying it as a flux for more refractory compounds, creating dense protective coatings. In addition, Li<sub>3</sub>BO<sub>3</sub> is a lithium ion conductor [10], and its molecular mass is smaller than that of LiCoO<sub>2</sub> and other cathode materials. Li<sub>3</sub>BO<sub>3</sub> coating also increases the concentration of Li<sup>+</sup> in the contact layer with electrolyte.

Most coating strategies are based on the sol-gel method or impregnation of cathode materials powders with salt solutions with subsequent drying and annealing [1–3, 5–7]. However, the application of lithium borates via solutions guarantees neither synthesis of the nominal composition of lithium borate nor the density of the coating after annealing at 500 °C. It can be assumed that addition and distribution of LiBO<sub>2</sub>, Li<sub>2</sub>B<sub>4</sub>O<sub>7</sub> or Li<sub>3</sub>BO<sub>3</sub> compounds in the cathode bulk with subsequent annealing at melting temperatures of the corresponding eutectics may cause positive effect.

For the production of cathode materials, different modifications of solid-phase and hydrothermal methods are usually employed [12]. In laboratory studies for the obtaining of the cathode materials, in particular, lithium cobaltite, combustion reactions [13-18] are more often used [19-24]. The attraction of solution combustion synthesis (SCS) reactions for industrial application is determined by the following characteristics:

1. cathode material can be produced almost without sewage;
2. energy consumption for the decomposition of precursors is reduced compared to conventional technologies, since the method employs internal exothermal processes requiring only relatively moderate energy consumption for evaporation of reaction solutions and preliminary heating of xerogel before the beginning of redox reaction;
3. dispersion and chemical activity of produced precursor may reduce the time of high-temperature annealing to attain the monophasic;
4. although the initial solutions contain nitrates, combustion proceeds with almost complete transformation of nitrogen dioxides into molecular nitrogen;
5. this method allows to control the dispersion of the material while reducing the costs for milling and lessening the risk of pollution of the material during milling.

However, in the  $\text{LiNO}_3\text{-Co}(\text{NO}_3)_2\text{-glycine}$  (urea) systems, a redox reaction of LCO formation proceeds intensely with outflow of a considerable part of precursor with effluent gases outside the reactor. Under stoichiometric combustion conditions, the combustion rate may have an explosive character. It is reasonable to expect that the described above effects detected under conditions of laboratory experiments will be multiply strengthened if the mass of the material is increased. This problem can be solved by using of less energetic fuel for controlled reduction of SCS rate, for example, sucrose, ammonium acetate starch, citric acid and oxalic acid [24-28].

In this paper, we report structural, morphological, dimensional and electrochemical characteristics of LCO powders produced in SCS reactions with glycine and citric acid with subsequent coating with fused lithium borate  $\text{Li}_3\text{BO}_3$ .

## 2. Experimental

### 2.1. Starting materials

For the combustion synthesis of LCO powders, cobalt(II) nitrate hexahydrate (99%) and cobalt(II) carbonate hydrate hydrate  $\text{CoCO}_3\cdot m\text{Co}(\text{OH})_2\cdot n\text{H}_2\text{O}$  (with cobalt content of 55.5%) (Ural Chemical Reagents Plant, Russia) were used as cobalt sources, and lithium carbonate (UNICHIM (Russia), 99%) was used as a source of lithium. Citric acid hydrate  $\text{H}_3\text{C}_6\text{H}_5\text{O}_7\cdot \text{H}_2\text{O}$  (Citrobel (Russia), 99.8%) and amino acetic acid (glycine)  $\text{H}_2\text{N}(\text{CH}_2)\text{COOH}$  (Kamhimkom (Russia), 98.5%) were used as fuel, while

double-distilled water served as a solvent for precursor solutions. The synthesis of lithium borate was carried out from boric acid (UNICHIM (Russia), 99.5%) and lithium carbonate (NPF Nevsky Chemist (Russia), 99.5 %).

### 2.2. Synthesis

Lithium nitrate combined with cobalt nitrate imparts excessive combustion intensity to SCS reactions. In the methods where glycine used as a fuel / reductant, the combustion rate during synthesis of cathode materials of LIB can be considerably decreased by replacing lithium nitrate by lithium carbonate or lithium citrate [24]. Besides, the reduction of the fraction of cobalt nitrate (oxidizer) due to its replacement by cobalt citrate also lowers the SCS intensity allowing the yield increasing of the resulting material [24].

In this work, we used one-step mode of LCO production. For this purpose, a 150 ml solution of cobalt nitrate ( $66.67 \text{ g/dm}^3 \text{ Co}$ ) and citric acid ( $237.5 \text{ g/dm}^3$ ) (solution 1) was placed into a  $2 \text{ dm}^3$  reactor, to which  $120 \text{ cm}^3$  lithium citrate solution ( $286.68 \text{ g/dm}^3 \text{ Li}_2\text{HC}_6\text{H}_5\text{O}_7$ ) was added. Cobalt (II) carbonate hydroxide hydrate and glycine successively added to the resulting solution (Table 1).

The reaction solution was heated on an electrical heater with a capacity of 1 kW (the temperature of the heater was  $550\text{--}600^\circ\text{C}$ ) for dehydration and initiation of SCS reaction. The produced LCO precursor was ground in a ball mill with grinding bodies made of stabilized zirconium oxide prior and between the annealing at  $650$ ,  $800$  and  $850^\circ\text{C}$ . The annealing duration at each stage was 10 h.

After certification, LCO powders were coated with fused  $\text{Li}_3\text{BO}_3$  (LBO) produced preliminarily in a solid-phase reaction using lithium carbonate and boric acid at  $560\text{--}600^\circ\text{C}$  for 35 h with intermediate grinding. 5 and 7 mass % of LBO were added to the initial LCO powder and mixed in a ball mill for 1 h, then they were annealed at  $750^\circ\text{C}$  for 5 h. After the first annealing, the LCO/LBO samples were repeatedly ground and annealed for the second time at  $750^\circ\text{C}$  for 5 h to produce better uniform coating.

### 2.3. Characterization of powder samples

The diffraction patterns of the powders were taken at room temperature with a Shumadzu XRD-700 ( $\text{Cu K}\alpha_1$  radiation,  $2\theta = 10\text{--}80^\circ$ ) diffractometer, equipped with PDF2 database. The refinement of the crystal structure according to the Rietveld method carried out using the software package FullProf [29]. SEM images obtained with a JEOL JSM 6390 LA microscope. Specific surface area ( $S$ ) of powders was determined by BET nitrogen desorption during heating in a SORBI N4.1 (Meta, Russia). The particle size distribution of the obtained powders was determined using a Horiba LA-950V2 laser particle meter.

### 2.4. Electrochemical measurements

The electrochemical properties of the LCO powder samples were studied using two-electrode pouch cells. The composite electrodes were prepared by inkjet printing of a ho-

mogenized mixture of the synthesized material, a conductive additive (acetylene black) and a binder (polyvinylidene fluoride dissolved in N-methyl-2-pyrrolidone) (weight ratio of solid components 80:10:10) onto an aluminum foil. The electrodes were compacted in a rolling mill and then dried under vacuum at 120 °C for 12 h. The area of the prepared electrode was of 2.25 cm<sup>2</sup>. The active material loading of the electrode was about 3–6 mg cm<sup>-2</sup>.

The electrochemical test cells Li|liquid electrolyte|LCO were assembled in an argon-filled MBraun LAB Star glove box with O<sub>2</sub> and H<sub>2</sub>O contents <0.1 ppm. Lithium foil (99.9 %, Alfa Aesar) was used as a counter electrode. Celgard 2300 film was used as a separator. The solution of 1 M LiPF<sub>6</sub> in ethylene carbonate (EC) and ethyl methyl carbonate (EMC) (1:1 vol.) (Sigma Aldrich) was used as the electrolyte. The residual water content in the electrolyte solution did not exceed 30 ppm.

Cycling performance and rate capability of the cathode half-cells were examined at 25 °C by galvanostatic charge-discharge curves measured with P-20X80 multichannel potentiostat (“Elins” LLC, Russia) in the voltage range of 2.7–4.3 vs. Li<sup>0</sup>/Li<sup>+</sup>. Current density varied from 0.1 to 0.5C.

### 3. Results and Discussion

SCS as the chosen LCO obtaining method allowed to increase the mass of the obtained product without growing the reaction temperature and rate, i.e. without discharge of the produced powder. Evaporation of the solution led to the formation of a semi-sphered dried gel covered with a violet film. The dry outer layer gradually closed the whole semi sphere, inside which a wet gel remained (Fig. 1a) also transforming gradually into dry precursor material. The redox reaction proceeded in the form of a heating wave (Fig. 1b) with low violet flame. There was no discharge of the material outside the reactor, and no visible traces of nitrogen dioxide were present. When the combustion was completed, a bulky flake black powder of LCO precursor was obtained.



**Fig. 1** Formation of the product in SCS reactions

The LCO powders obtained after combustion possessed high dispersion and revealed chemically non-equilibrium state due to incomplete crystal lattice formation processes. This is connected with a short combustion time (the reaction mass was in the high-temperature region for less than 3–5 min); low density of the material (as a result of large amount of gaseous products) hampers the completion of diffusion processes during LCO formation. Usually, the SCS process is supplemented with high-temperature annealing, in this case in the range of 650–850 °C, to remove carbon-containing impurities and form the LCO crystal structure (Table 1, Fig. 2). Upon annealing, the crystal lattice parameters of the produced LCO corresponded to the literature data [30]. Reflections of the fused LBO coating were not recorded, probably due to its glassy character.

The performed sedimentation analysis revealed that LCO represents finely dispersed powders forming agglomerates with the maximal diameter,  $D_{\max}$ , of <30 μm (Table 2) and the average particle diameter,  $D_{\text{av}}$ , of 8.4–11.5 μm.

**Table 1** LCO crystal lattice parameters after annealing at 850 °C

Sample	$a$ , Å	$c$ , Å	$V$ , Å <sup>3</sup>	$R_1$	$R_2$
1	2.8165 (2)	14.0604 (21)	96.5921	1.72	0.57
[30]	2.81619	14.05586	96.5382	1.35	0.44

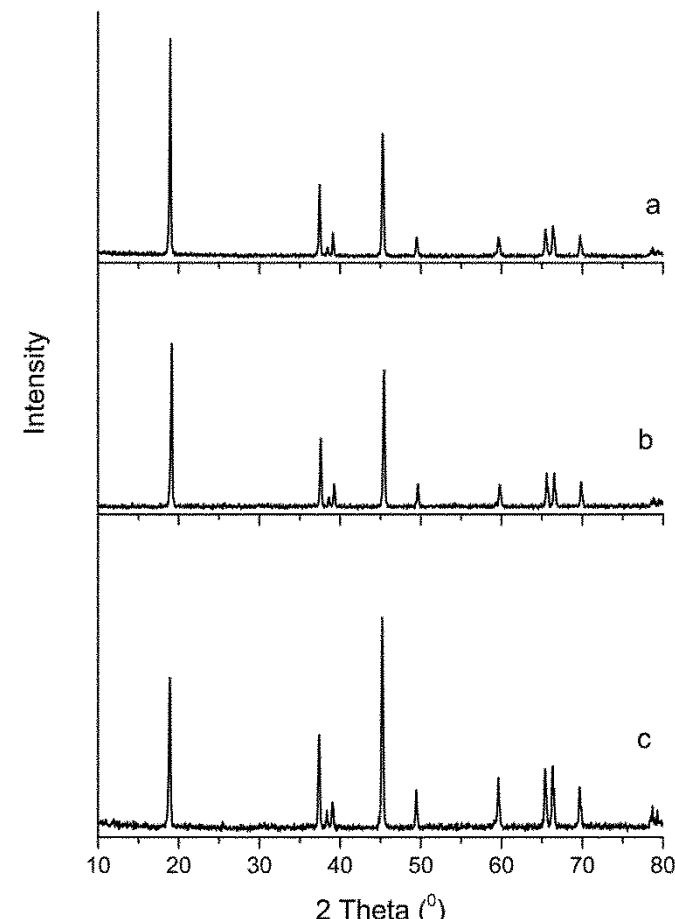


**Fig. 2** X-ray diffraction patterns of (a) LCO, (b) LCO+5% LBO, (c) LCO +7% LBO

The fraction of particles less than 5  $\mu\text{m}$  is rather large, from 6 to 30%. The application of borate coating considerably changes the particle size distribution in the material;  $D_{\text{av}}$  increases to 11–45  $\mu\text{m}$  and depends explicitly on the milling conditions and load. The fraction of particles with a diameter less than 5  $\mu\text{m}$  decreases to 1.1–1.3% (Table 2), which should have a positive effect on the cathode stability during the interaction with electrolyte. However, the presence of aggregate fractions larger than 30  $\mu\text{m}$  required the classification of powders before applying the electrode mass.

Coating of LCO with a layer of fused lithium borate practically does not change the specific surface of the material (Table 2), remaining equal to 0.8–0.98  $\text{m}^2/\text{g}$ . This value is larger than the traditional values for commercial cathode materials, 0.4–0.6  $\text{m}^2/\text{g}$ , but possibly has positive impact on the electrochemical characteristics during cycling. The advantage of coating by fusion is that fusion and spreading of LBO on the surface of LCO particles and agglomerates decreases the coating thickness and increases the probability of connection of small particles, reducing the influence of electrolyte.

The sizes of LCO-LBO powders are slightly larger than the base (LCO) particles, it contain a smaller percent of fine fractions due to enhanced sintering into agglomerates and additional annealing time (growth of primary crystallites) (Fig. 3).

The charge-discharge characteristics of cathode materials based on LCO were studied in the potential range of 2.75–4.3 V vs Li/Li<sup>+</sup>. The charge and discharge rate of the first 10 cycles were 0.1C. Then, at the same charge rate, 10 cycles performed with a discharge rate of 0.2C, 0.5C and again 0.1C. Fig. 4 shows the capacity dependences on the cycle number based on a series of powders: LCO, LCO + 5% LBO and LCO + 7% LBO as samples with the most stable characteristics.

The discharge capacity of the sample without coating at the first cycle was 166 mAh/g. A significant increase of the discharge capacity (up to 185 mAh/g) was achieved by using a 5% LBO coating. When the LBO content of the sample increases to 7%, the discharge capacity drops to

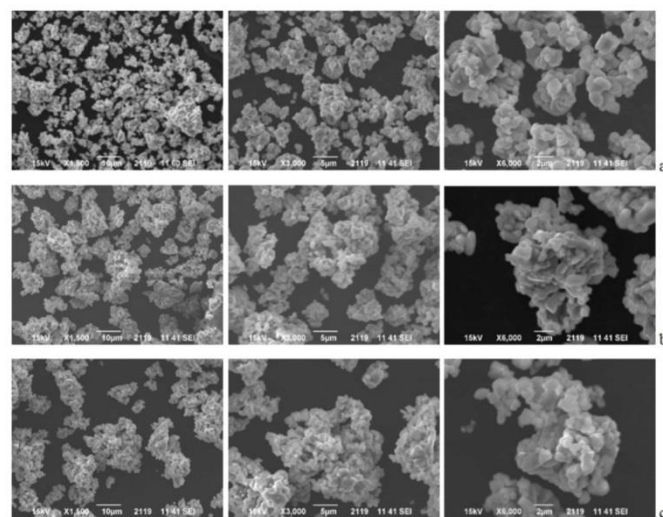


**Fig. 3** Morphology of (a) LCO, (b) LCO+5% LBO, (c) LCO +7% LBO powders

164 mAh/g. The negative effect probably related to the increasing thickness of the coating layer and/or the formation of less conducting glasses during the interaction of fused LBO with LCO.

All samples retain 94, 93 and 93% of the original discharge capacity after 40 cycles when the cycle rate returned to the original rate 0.1C. In addition, the coulomb efficiency of these samples is more than 99% throughout all 40 charge-discharge cycles (Table 3).

Fig. 5 shows the charge-discharge curves of the first cycle for LCO, LCO+5% LBO and LCO +7% LBO. The type of the charge-discharge curves corresponds to the typical charge-discharge curves obtained for lithium cobaltate-based cathodes [21, 31, 32].

The charge-discharge curves have a plateau at a potential of 3.9 V and two small quasi-plateaus at 4.1 and 4.2 V. These plateaus correspond to the peaks on the cyclic voltammograms (Fig. 6). According to the literature data [32–36], the main peak at 3.9 V is related to the first order transition from LCO to  $\text{Li}_{0.8}\text{CoO}_2$ ; the two less pronounced peaks at ~4.06 and ~4.17 V are associated with phase transitions to the monoclinic structure and back to the hexagonal structure.

**Table 2** The results of sedimentation analysis of LCO-LBO powders

LCO - LBO	$D_{\text{av}}$ , $\mu\text{m}$	$D_{\text{med}}$ , $\mu\text{m}$	Fraction < 5 $\mu\text{m}$ , %	$D_{\text{max}}$ , $\mu\text{m}$	Fraction >30 $\mu\text{m}$ , %	Fraction 30–100 $\mu\text{m}$ , %	$S$ , $\text{m}^2/\text{g}$
LCO	8.4	8.2	13.5	30	0	0	$0.82 \pm 0.02$
LCO+5% LBO	43	14	1.3	300	24	11	$0.86 \pm 0.04$
LCO+7% LBO	37	16	1.1	300	29	19	$0.92 \pm 0.03$

**Table 3** The cyclic performance of LCO powders in the range of 2.75–4.3 V at different rates

	Discharge capacity, mAh/g (cycle number)				Coulomb efficiency, % (cycle number)			
	0.1C (10)	0.2C (20)	0.5C (30)	0.1C (40)	(10)	(20)	(30)	(40)
LCO	162	158	145	153	99.5	99.7	99.9	99.1
LCO+5% LBO	185	180	173	172	99.5	99.7	99.9	99.1
LCO+7% LBO	162	158	152	150	99.5	99.7	99.9	99.1

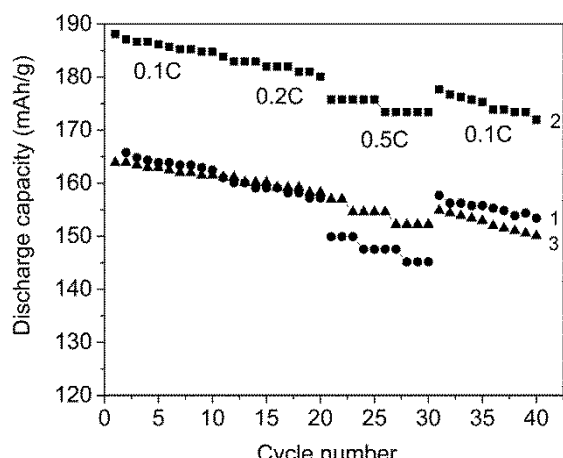


Fig. 6 Cyclic performance of the LCO samples:  
1 – LiCoO<sub>2</sub>, 2 – LiCoO<sub>2</sub> + 5% LBO, 3 – LiCoO<sub>2</sub> + 7% LBO

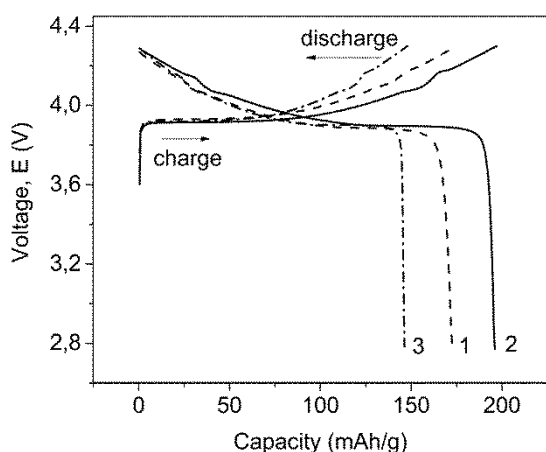


Fig. 6 Charge-discharge curves of: 1 – LCO, 2 – LCO+5% LBO, 3 – LCO +7% LBO

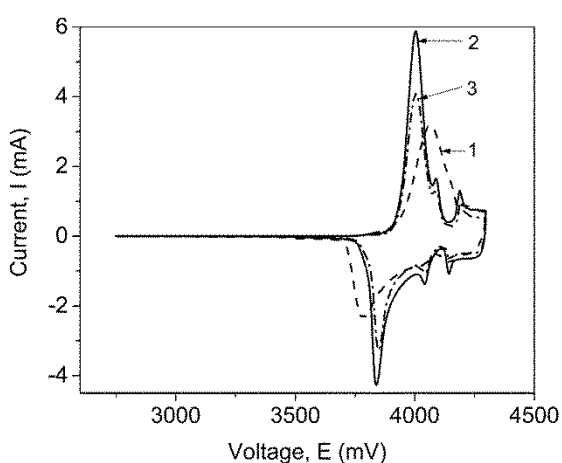


Fig. 6 Cyclic voltammograms of: 1 – LCO, 2 – LCO+5% LBO, 3 – LCO +7% LBO

Based on the obtained data, it is possible to conclude that borate coating does not affect the electrode polarization, as the discharge plateau does not change.

According to the data obtained by the cyclic voltammetry method and based on the peaks intensity on the cyclic voltammograms, one may conclude that due to the pres-

ence of 5 mass % of LBO coating on the lithium cobaltite surface, it is possible to activate the electrode surface and increase the reversibility of lithium introduction and extraction processes into the electrode. Wider peaks for the uncoated sample may be an indication of inhibition of lithiation and delithiation processes as compared to the modified samples. Consequently, the presence of LBO coating may affect the rate of lithium diffusion into cathode material particles.

Thus, borate coating increases the stability of cobaltite cycling at elevated rates. When the rate increases to 0.5C, the capacity falls by 4% for coated samples and by 8% for uncoated samples.

#### 4. Conclusions

The best electrochemical characteristics, discharge capacity of 185 mAh/g at 0.1C and coulomb efficiency of 99.1% after 40 cycles, were demonstrated by the sample obtained in the SCS reaction of cobalt nitrate with lithium citrate and glycine and coated with 5 mass % of LiBO<sub>3</sub>. Fused LiBO<sub>3</sub> coating increases the cobaltate cycling stability at elevated rates.

#### Acknowledgments

The work was performed in accordance with the state assignments of the Institute of Chemistry of Solids of the Ural Branch of the RAS, No. AAAA-A19-119031890026-6 and No. AAAA-A19-119102990044-6, the state assignment of the Institute of Problems of Chemical Physics of the RAS, No. AAAA-A19-119061890019-5, and Thematic map No. 0089-2019-0007 «Functional materials for chemical power sources».

#### References

1. Blomgren GE. The development and future of lithium ion batteries. *J Electrochem Soc Jpn.* 2017;164:A5019–25. doi:[10.1149/2.025170jes](https://doi.org/10.1149/2.025170jes)
2. Maximov MYu, Popovich AA, Rumyantsev AM. Influence of passivation coatings synthesized by atomic layer deposition on Li-Ion Batteries cathode cycle life advanced. *Materials Research.* 2015;1120-1121:730-4. doi:[10.4028/www.scientific.net/AMR.1120-1121.730](https://doi.org/10.4028/www.scientific.net/AMR.1120-1121.730)
3. Fu LJ, Liu H, Li C, Wu YP, Rahm E, Holze R, Wu HQ. Surface modifications of electrode materials for Lithium Ion Batteries. *Solid State Sci.* 2006;8:113–28. doi:[10.1016/j.solidstatesciences.2005.10.019](https://doi.org/10.1016/j.solidstatesciences.2005.10.019)
4. George SM, Ott AW, Klaus JW. Surface chemistry for atomic layer growth. *J Phys Chem.* 1996;100:13121–31. doi:[10.1021/jp9536763](https://doi.org/10.1021/jp9536763)
5. Zhou A, Wang W, Liu Q, Wang Y, Yao X, Qing F, Li E, Yang T, Zhang L, Li J. Stable, fast and high-energy-density LiCoO<sub>2</sub> cathode at high operation voltage enabled by glassy B<sub>2</sub>O<sub>3</sub> modification. *J Power Sources.* 2017;362:131–9. doi:[10.1016/j.jpowsour.2017.06.050](https://doi.org/10.1016/j.jpowsour.2017.06.050)
6. Nagasubramanian A, Yu DYW, Hostler H, Srinivasan M. Enhanced cycling stability of 0-LiMnO<sub>2</sub> cathode modified by lithium boron oxide coating for lithium-ion batteries. *J Solid State Electrochem.* 2014;18:1915–22. doi:[10.1007/s10008-014-2421-3](https://doi.org/10.1007/s10008-014-2421-3)

7. Tan SY, Wang L, Bian L, Xu JB, Ren W, Hu PF, Chang AM. Highly enhanced low temperature discharge capacity of  $\text{LiNi}_{1/3}\text{Co}_{1/3}\text{Mn}_{1/3}\text{O}_2$  with lithium boron oxide glass modification. *J Power Sources.* 2015;277:139–46.  
doi:[10.1016/j.jpowsour.2014.11.149](https://doi.org/10.1016/j.jpowsour.2014.11.149)
8. Chen S, Chen L, Li Y, Su Y, Lu Y, Bao L, Wang J, Wang, Wu F. Synergistic effects of stabilizing the surface structure and lowering the interface resistance in improving the low-temperature performances of layered lithium-rich materials. *ACS Appl Mater Interfaces.* 2017;9:8641–8.  
doi:[10.1021/acsami.6b13995](https://doi.org/10.1021/acsami.6b13995)
9. Ohta S, Komagata S, Seki J, Saeki T, Morishita S, Asaoka T. All-solid-state lithium ion battery using garnet-type oxide and  $\text{Li}_3\text{BO}_3$  solid electrolytes fabricated by screen-printing. *J Power Sources.* 2013;238:53–6.  
doi:[10.1016/j.jpowsour.2013.02.073](https://doi.org/10.1016/j.jpowsour.2013.02.073)
10. Jinilian L, Xianming W, Shang C, Jianben L, Zeqiang H. Enhanced high temperature performance of  $\text{LiMn}_2\text{O}_4$  coated with  $\text{Li}_3\text{BO}_3$  solid electrolyte. *Bull Mater Sci.* 2013;36:687–91.  
doi:[10.1007/s12034-013-0513-9](https://doi.org/10.1007/s12034-013-0513-9)
11. Ferreira E, Lima M, Zanotto E. DSC Method for determining the liquidus temperature of glass-forming systems. *J Am Ceram Soc.* 2010;93:3757–63.  
doi:[10.1111/j.1551-2916.2010.03976.x](https://doi.org/10.1111/j.1551-2916.2010.03976.x)
12. Antolini E.  $\text{LiCoO}_2$ : formation, structure, lithium and oxygen nonstoichiometry, electrochemical behaviour and transport properties. *Solid State Ionics.* 2004;170:159–71.  
doi:[10.1016/j.ssi.2004.04.003](https://doi.org/10.1016/j.ssi.2004.04.003)
13. Mukasyan A, Epstein P, Dinka P. Solution combustion synthesis of nanomaterials. *Proc Combust Inst.* 2007;31:1789–95.  
doi:[10.1016/j.proci.2006.07.052](https://doi.org/10.1016/j.proci.2006.07.052)
14. Mimani T, Patil K. Solution combustion synthesis of nanoscale oxide and their composites. *Mater Phys Mech.* 2001;4:134–7.
15. González-Cortés S, Imbert F. Fundamentals, properties and applications of solid catalysts prepared by solution combustion synthesis (SCS). *Appl Catal A: General.* 2013;452:117–31.  
doi:[10.1016/j.apcata.2012.11.024](https://doi.org/10.1016/j.apcata.2012.11.024)
16. Deganello F, Tyagi A. Solution combustion synthesis, energy and environment: Best parameters for better materials. *Prog Cryst Growth Charact Mater.* 2018;64:23–61.  
doi:[10.1016/j.pcrysgrow.2018.03.001](https://doi.org/10.1016/j.pcrysgrow.2018.03.001)
17. Jayasankar K, Pandey A, Mishra B, Das S. Mixed fuel synthesis of  $\text{Y}_2\text{O}_3$  nanopowder and their applications as dispersed in ODS steel. *Adv Powder Technol.* 2015;26:1306–13.  
doi:[10.1016/j.apt.2015.07.003](https://doi.org/10.1016/j.apt.2015.07.003)
18. Zhuravlev V, Pachuev A, Nefedova K, Ermakova L. Solution combustion synthesis of  $\text{LiNi}_{1/3}\text{Co}_{1/3}\text{Mn}_{1/3}\text{O}_2$  as a cathode material for lithium-ion batteries. *Int J Self-Propagating High-Temp Synth.* 2018;27:154–61.  
doi:[10.3103/S1061386218030147](https://doi.org/10.3103/S1061386218030147)
19. Santiago E, Andrade A, Paiva-Santos C, Bulhoës L. Structural and electrochemical properties of  $\text{LiCoO}_2$  prepared by combustion synthesis. *Solid State Ionics.* 2003;158:91–102.  
doi:[10.1016/S0167-2738\(02\)00765-8](https://doi.org/10.1016/S0167-2738(02)00765-8)
20. Kalyani P, Kalaiselvi N, Muniyandi N. A new solution combustion route to synthesize  $\text{LiCoO}_2$  and  $\text{LiMnO}_2$ . *J Power Sources.* 2002;111:232–8. doi:[10.1016/S0378-7753\(02\)00307-5](https://doi.org/10.1016/S0378-7753(02)00307-5)
21. Yoon W, Kim K. Synthesis of  $\text{LiCoO}_2$  using acrylic acid and its electrochemical properties for Li secondary batteries. *J Power Sources.* 1999;81–82:517–23.  
doi:[10.1016/S0378-7753\(98\)00226-2](https://doi.org/10.1016/S0378-7753(98)00226-2)
22. Rodrigues S, Munichandraiah N, Shukla A. Novel solution-combustion synthesis of  $\text{LiCoO}_2$  and its characterization as cathode material for lithium-ion cells. *J Power Sources.* 2001;102:322–5. doi:[10.1016/S0378-7753\(01\)00770-4](https://doi.org/10.1016/S0378-7753(01)00770-4)
23. Hobosyana M, Kharatyan S, Khachatryan H, Grigoryan N. Combustion synthesis of lithium cobaltate. *Int J Self-Propagating High-Temp Synth.* 2011;20:107–12.  
doi:[10.3103/S1061386211020075](https://doi.org/10.3103/S1061386211020075)
24. Zhuravlev V, Shikhovtseva A, Ermakova L, Evshchik E, Sherstobitova E, Novikov D, Bushkova O, Dobrovolsky Y. Solution combustion synthesis of lithium cobalt oxide – cathode material for lithium-ion batteries. *Int J Electrochem Sci.* 2019;14:2965–83. doi:[10.20964/2019.03.79](https://doi.org/10.20964/2019.03.79)
25. Khalilullin S, Zhuravlev V, Ermakova L, Buldakova L, Yanchenko M, Porotnikova N. Solution combustion synthesis of  $\text{ZnO}$  using binary fuel (glycine + citric acid). *Int J Self-Propagating High-Temp Synth.* 2019;28:226–32.  
doi:[10.3103/S1061386219040058](https://doi.org/10.3103/S1061386219040058)
26. Han C, Zhu C, Saito G, Akiyama T. Glycine/sucrose-based solution combustion synthesis of high-purity  $\text{LiMn}_2\text{O}_4$  with improved yield as cathode materials for lithium-ion batteries. *Adv Powder Technol.* 2015;26:665–71.  
doi:[10.1016/j.apt.2015.01.019](https://doi.org/10.1016/j.apt.2015.01.019)
27. Aruna S, Rajam K. Mixture of fuels approach for the solution combustion synthesis of  $\text{Al}_2\text{O}_3\text{-ZrO}_2$  nanocomposite. *Mater Res Bull.* 2004;39:157–67.  
doi:[10.1016/j.materresbull.2003.10.005](https://doi.org/10.1016/j.materresbull.2003.10.005)
28. Bai J, Liu J, Li C, Li G, Du Q. Mixture of fuels approach for solution combustion synthesis of nanoscale  $\text{MgAl}_2\text{O}_4$  powders. *Adv Powder Technol.* 2011;22:72–6.  
doi:[10.1016/j.apt.2010.03.013](https://doi.org/10.1016/j.apt.2010.03.013)
29. Rodríguez-Carvajal J. Recent advances in magnetic structure determination by neutron powder diffraction. *Physica B.* 1993;192:55–69. doi:[10.1016/0921-4526\(93\)90108-1](https://doi.org/10.1016/0921-4526(93)90108-1)
30. Xuanye Y, Hongge Y, Jihua C, Mao H, Feng X, Zhengfu Z, Hongmei X. Solid state synthesis of ultrafine- $\text{LiCoO}_2$  by enhanced thermal decomposition of carbonate precursors followed by double-calcining. *Solid State Ionics.* 2016;289:159–67. doi:[10.1016/j.ssi.2016.03.005](https://doi.org/10.1016/j.ssi.2016.03.005)
31. Xie J, Imanishi N, Hirano A, Matsumura M, Takeda Y, Yamamoto O. Kinetics investigation of a preferential (104) plane oriented  $\text{LiCoO}_2$  thin film prepared by RF magnetron sputtering. *Solid State Ionics.* 2007;178:1218–24.  
doi:[10.1016/j.ssi.2007.06.007](https://doi.org/10.1016/j.ssi.2007.06.007)
32. Choi Y, Pyun S, Bae J, Moon S. Effects of lithium content on the electrochemical lithium intercalation reaction into  $\text{LiNiO}_2$  and  $\text{LiCoO}_2$  electrodes. *J Power Sources.* 1995;56:25–30.  
doi:[10.1016/0378-7753\(95\)80004-Z](https://doi.org/10.1016/0378-7753(95)80004-Z)
33. Reimers JN, Dahn JR. Electrochemical and in situ X-ray diffraction studies of lithium intercalation in  $\text{Li}_x\text{CoO}_2$ . *J Electrochem Soc.* 1992;139:2091–7. doi:[10.1149/1.2221184](https://doi.org/10.1149/1.2221184)
34. Antolini E.  $\text{LiCoO}_2$ : formation, structure, lithium and oxygen nonstoichiometry, electrochemical behaviour and transport properties. *Solid State Ionics.* 2004;170:159–71.  
doi:[10.1016/j.ssi.2004.04.003](https://doi.org/10.1016/j.ssi.2004.04.003)
35. Amatucci G, Tarascon J, Klein L.  $\text{CoO}_2$ , the end member of the  $\text{Li}_x\text{CoO}_2$  solid solution. *J Electrochem Soc.* 1996;143:1114–23.  
doi:[10.1149/1.1836594](https://doi.org/10.1149/1.1836594)
36. Ohzuku T, Ueda A. Solid-state redox reactions of  $\text{LiCoO}_2$  ( $\text{R}3\text{m}$ ) for 4 volt secondary lithium cells. *J Electrochem Soc.* 1994;141:2010–5. doi:[10.1149/1.2059267](https://doi.org/10.1149/1.2059267)